Potts model on infinitely ramified Sierpinski-gasket-type fractals and algebraic order at antiferromagnetic phases

Fortunato S. de Menezes and Aglaé C. N. de Magalhães
Centro Brasileiro de Pesquisas Físicas, Rua Dr. Xavier Sigaud 150, 22290 Rio de Janeiro, Brazil
(Received 12 November 1991; revised manuscript received 16 June 1992)

We propose families of infinitely ramified fractals, which we call the m-sheet Sierpinski gasket with side b $[(m\mathrm{SG})_b]$, on which the q-state Potts model can be exactly solvable through a real-space renormalization-group (RSRG) technique for which there are phase transitions at *finite* temperatures for $m > 1$. We also propose, within a cell-to-cell RSRG scheme, a criterion for a suitable choice of cells in the study of antiferromagnetic (AF) classical spin models defined on (or approximated by) multirooted hierarchical lattices, and apply it for the AF Potts model on some $(m\mathrm{SG})_b$ fractals. Concerning the Ising model on the $(m\mathrm{SG})_2$ family, we obtain the *exact* para (P)–ferromagnetic (F) critical temperature as a function of m and verify that, for $m = 1$ and 2, there is no AF order (not even at zero temperature). We calculated the *exact* P-F and possibly exact P-AF critical frontiers and the corresponding correlation-length critical exponents for $q = 2$-, 3-, and 4-state Potts model on the $(m\mathrm{SG})_4$. The AF $q = 2$ and 4 cases have highly degenerate ground states and each one presents, above a certain critical fractal dimension $D_f^c(q,m)$, an unusual low-temperature phase whose attractor occurs at a non-null temperature. For $q = 2$ and $D_f(2,m) \geq 5.1$, we prove that the correlations have a power-law decay with distance along this entire phase.

I. INTRODUCTION

Gefen, Mandelbrot, and Aharony[1] presented the first systematic study of critical phenomena on fractals. Since then, much attention has been paid to the study of spin models on fractals[2–12] and, in particular, on hierarchical lattices (HL).[13–17] Many renormalization-group treatments which are intended to approximate spin systems on Bravais lattices become exact if the spins are, instead, placed on an appropriate HL. Different spin models have been exactly solved on bond hierarchical lattices such as, for example, the Ising model,[15,18–20] the Potts model,[21,22] the complete Blume-Emery-Griffths model,[23,24] the discrete cubic model,[25] the symmetric Ashkin-Teller model,[26] the Z(6) model,[27] and they present phase transitions at finite temperature. But on other fractal lattices, despite the fact that a number of different models have been exactly solved (see, for example, Refs. 2, 3, and 10), as far as we know, there are no exact solutions for the case of finite and short-range interactions which exhibit phase transition at a non-null temperature. The existence of such examples would certainly contribute to a better understanding of critical phenomena on these scale (but not translationally) invariant lattices.

In this paper we propose families of deterministic fractals (the m-sheet Sierpinski gaskets with side b) on which the q-state Potts model (see Ref. 28) can be *exactly solvable* and which presents phase transitions at *finite* temperatures for $m > 1$. These fractals constitute hierarchical lattices on which the aggregated objects are triangles instead of bonds as in bond hierarchical lattices. Due to their hierarchical character, the real-space renormalization-group (RSRG) employed here provides the *exact* para (P)–ferromagnetic (F) critical frontiers and the corresponding correlation-length critical exponents $\nu_T^{\mathrm{F}}(m)$.

For the antiferromagnetic (AF) Potts model, one has to be very cautious when a negative coupling constant changes sign under the first scaling leading, thus, to a renormalized ferromagnetic coupling in all subsequent iterations. Our interpretation of this result is that the symmetries of the AF ground state are not being preserved under renormalization and that it is essential to choose sufficiently large cells (which appear in two subsequent steps of construction of the fractal) which conserve these symmetries. This point has been neglected on Migdal-Kadanoff-like HL with even chemical distance[29,30] and, for $q = 2$, on the Sierpinski gasket ($b = 2$, $m = 1$).[9,11,12] Herein we discuss, within a cell-to-cell RSRG scheme where the spin states on the roots of the cells are fixed under renormalization, this point and propose a criterion for a suitable choice of cells in the study of AF classical spin models defined on HL (or on Bravais lattices which are approximated by these). Applying this criterion, we obtained the P-AF phase boundaries and their respective critical exponents $\nu_T^{\mathrm{AF}}(m)$, which we expect to be *exact,* for Potts antiferromagnets on the m-sheet Sierpinski-gasket families [which we shall refer hereafter to as $(m\mathrm{SG})_b$].

Another interesting feature of the AF Potts model on the $(m\mathrm{SG})_b$ fractals is the appearance, above a certain critical fractal dimension $D_f^c(q,m)$, of an unusual low-temperature phase in which the correlations have a power-law decay with distance. Such systems have a highly degenerate ground state which generates a nonzero entropy per site at zero temperature, violating

thus the third law of thermodynamics. This residual entropy appears also, for example, in AF Potts models on systems like bipartite lattices (for $q \geq 3$), fcc lattice [for $q \geq 2$ (Ref. 31)], a decorated square lattice,[32] and some fractals.[6,9,11,12] If one applies to such systems an argument similar to that of Wannier,[33] one would expect no long-range order of the usual type. But, after Berker and Kadanoff[34] suggested that such systems may present a distinctive low-temperature phase with algebraic decay of correlations, much work has been done[35,31,36,37,28,38,6,39,40,30] looking for this phase. For instance, in the case of the ($q=3$)-state Potts model on the bipartite cubic lattice, there are evidences that such a phase exists.[39,40] In Ref. 39, this model was examined by Monte Carlo lattices of sizes up to $15\times15\times16$ with periodic boundary condition simulations. From an analysis of the behavior of the probabilities of occurrence of fixed states on each sublattice, and from the study of a lattice-size dependence of the order-parameter fluctuations, the author concluded that, below a certain critical temperature $T_c \neq 0$, the order parameter might be zero and that the correlations have a power-law decay. Wang, Swendsen, and Kotecky,[40] using a more efficient Monte Carlo method, confirmed this algebraic decay (through the divergence of the staggered susceptibility) although disagreed with the vanishing of the order parameter. In the case of fractals, there are also evidences of the existence of an unusual phase.[6,30] Riera[6] studied, through the approximate bond-moving Migdal-Kadanoff scheme, the phase diagrams of the AF Potts model on Sierpinski carpet and pastry-shell families. She found, in some cases, attractors of low-temperature phases at non-null temperatures—a feature which also appears in Berker and Kadanoff's RSRG picture.[34] This characteristic was also found, in an exact way, by Qin and Yang[30] in this model laid on some Migdal-Kadanoff HL types. Although, in some cases, there are evidences that an unusual phase exists (as in the above-mentioned examples), there is no proof, as far as we know, that the correlations decay algebraically along this phase. Herein we prove this for the Ising antiferromagnet on the $(m\mathrm{SG})_4$ for $m \geq 116$ (and hence for fractal dimensions $D_f \geq 5.1$). The existence of an attractor at finite temperature ($T \neq 0$) for the $q=4$ AF Potts model with two- and three-spin interactions on the $(m\mathrm{SG})_4$ with $m \geq 17$ ($D_f \geq 3.7$) indicates that such a phase also appears in this case.

The outline of this paper is as follows. In Sec. II, we define the fractal families $(m\mathrm{SG})_b$ and the q-state Potts model with two- and three-spin interactions. In Sec. III, we present the two-parameter RSRG formalism (valid for $q \neq 2$), as well as that with one parameter suitable for treating the Ising model without three-spin interactions. In Sec. IV, we propose a criterion for a convenient choice of cells in the study of AF classical spin models defined on (or approximated by) HL. This criterion is a generalization of the one derived in this section from a mathematical analysis at $T=0$ of the most general form that the mentioned one-parameter RSRG can have. The appearance of an unusual attractor at a finite temperature emerges naturally from such analysis. The application of this criterion led to the results reported in Sec. V for the Ising model on the $(m\mathrm{SG})_2$ and for the $q=2$-, 3- and 4-state Potts model on the $(m\mathrm{SG})_4$. Finally, in Sec. VI, the conclusions are given.

II. MODEL

The m-sheet Sierpinski gasket $(m\mathrm{SG})_b$ is a generalization of the two-dimensional case of the Sierpinski-gasket family proposed by Hilfer and Blumen.[41] The spectral dimension,[41,42] moments of a voltage distribution in resistor networks,[43] criticality of self-avoiding walks,[44] residual entropy,[9,45] and other thermodynamical properties[9] of the Ising model have been studied for the $(1\mathrm{SG})_b$ family. Each member of the $m=1$ family has a generator $G(b)$ (b is an integer) constituted by an equilateral triangle of side length b which contains $b(b+1)/2$ upward oriented triangles of unit side. The $(m\mathrm{SG})_b$ fractal (where b and m are fixed) has a generator $G(b,m)$ (see Fig. 1) which

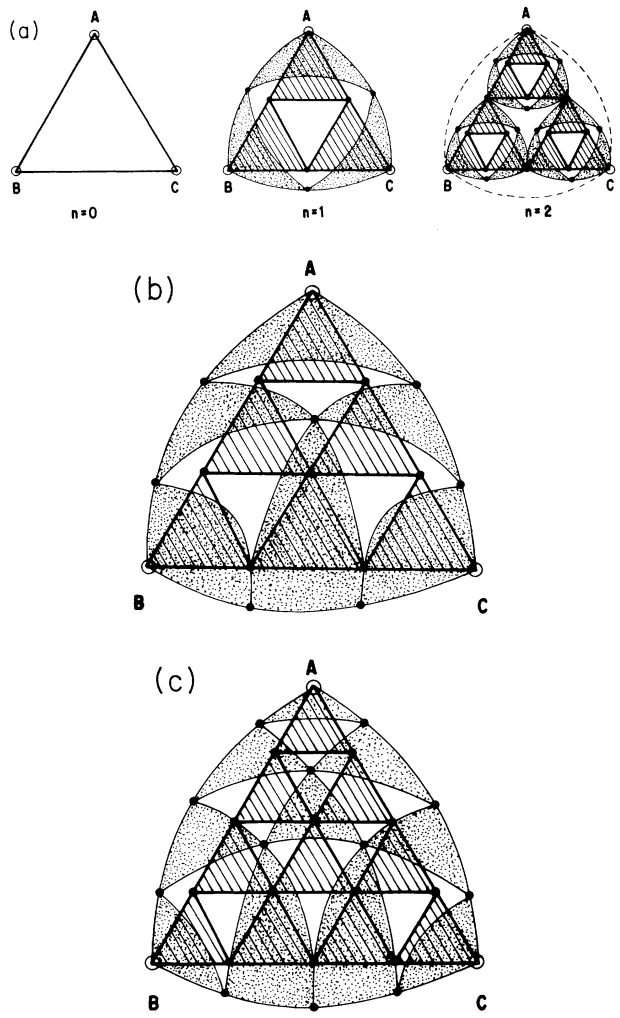

FIG. 1. (a) The first three stages (n) of construction of the $(2\mathrm{SG})_2$ fractal. The second sheet of the $n=2$ stage connected to A, B, and C is represented by just a single dashed line for visual purposes. (b) The generator ($n=1$) stage of the $(2\mathrm{SG})_3$. (c) The generator of the $(2\mathrm{SG})_4$. The roots and internal sites are represented by open and solid points, respectively.

consists of m structures topologically similar to $G(b)$ connected only at three external sites A, B, and C (hereafter called roots). $G(b,m)$ constitutes the $n=1$ stage of construction of the $(m\mathrm{SG})_b$ fractal obtained in the $n\to\infty$ limit. Any stage is obtained from the previous one by replacing each upward-oriented triangle of each sheet by the respective generator, and leaving the downward triangles empty [see, for $m=2$, Fig. 1(a)]. In each step, $mb(b+1)/2$ new units are generated, leading, thus, to a fractal dimension D_f given by

$$D_f=\frac{\ln[b(b+1)m/2]}{\ln b} . \tag{1}$$

One can easily show that in each stage (n) the order of ramification[46] R_n satisfies the recursive equation $R_n(m)=mR_{n-1}$, where $R_1(m)>1$ for all m. Therefore, unlike the $m=1$ case which is finitely ramified,[41] the $(m\mathrm{SG})_b$ has an infinite order of ramification for $m>1$. The particular case $(2\mathrm{SG})_2$ was introduced[13] as an example of a HL in which the aggregated objects are more complex than bonds.

At each site of the $(m\mathrm{SG})_b$ fractal with fixed b and m, we associate a Potts spin variable $\sigma_i=1,2,\ldots,q$ and consider the q-state Potts model with two-(J_2) and three-(J_3) spin interactions described by the following dimensionless Hamiltonian:

$$\beta\mathcal{H}=-K_2\sum_{\langle i,j\rangle}\delta(\sigma_i,\sigma_j)-K_3\sum_{\langle i,j,l\rangle}\delta(\sigma_i,\sigma_j,\sigma_l) , \tag{2}$$

where $\beta=1/K_bT$, $K_i=J_i\beta$ $(i=2,3)$, and $\delta(\sigma_i,\ldots,\sigma_l)=1(0)$, if $\sigma_i=\cdots=\sigma_l$ (otherwise). The first sum is over all nearest-neighbor (NN) pairs of spins and the second one is over the spins on all the upward-pointing triangles. We consider here either positive or negative values for both coupling constants.

III. FORMALISM

Let us now define our renormalization group. For this, we perform a scale transformation from one cell of side b to another of smaller side b' together with a renormalization of the parameters K_2 and K_3. The last step consists in summing over the spin states of the b and b' cells, with the restriction that the spins (σ_A, σ_B, and σ_C) on the roots are held in fixed states α, β and γ, namely,

$$W_m(\alpha,\beta,\gamma)=DW'(\alpha,\beta,\gamma) , \tag{3}$$

where

$$\begin{aligned}W_m(\alpha,\beta,\gamma)&\equiv\sum_{\{\sigma_i\}}\delta(\sigma_A,\alpha)\delta(\sigma_B,\beta)\delta(\sigma_C,\gamma)e^{-\beta\mathcal{H}}\\&=Z\langle\delta(\sigma_A,\alpha)\delta(\sigma_B,\beta)\delta(\sigma_C,\gamma)\rangle_{b\text{cell}}\\&=Zp(\sigma_A=\alpha,\sigma_B=\beta,\sigma_C=\gamma) ,\end{aligned} \tag{4}$$

$$\begin{aligned}W'(\alpha,\beta,\gamma)&\equiv\sum_{\{\sigma'_i\}}\delta(\sigma'_A,\alpha)\delta(\sigma'_B,\beta)\delta(\sigma'_C,\gamma)e^{-\beta\mathcal{H}'}\\&=Z'\langle\delta(\sigma'_A,\alpha)\delta(\sigma'_B,\beta)\delta(\sigma'_C,\gamma)\rangle_{b'\text{cell}}\\&=Z'p'(\sigma'_A=\alpha,\sigma'_B=\beta,\sigma'_C=\gamma) ,\end{aligned} \tag{5}$$

where $\langle\cdots\rangle$ represents the standard thermal average, and D is a constant due to the renormalization of the zero energy. Z and Z' are the respective partition functions of the nonrenormalized (b cell) and the renormalized (b') one. $p(\sigma_A=\alpha,\sigma_B=\beta,\sigma_C=\gamma)$ is the probability that the rooted spins σ_A, σ_B, and σ_C of the b cell are in the respective states α, β and γ; a similar definition follows for $p'(\sigma'_A=\alpha,\sigma'_B=\beta,\sigma'_C=\gamma)$ in the renormalized cell. Due to the symmetry of the considered cell, it appears only three different "constrained" partition functions $W_m(\alpha,\beta,\gamma)$: $W_{\mathrm{F}}^{(m)}\equiv W_m(\alpha,\alpha,\alpha)$, $W_{\mathrm{I}}^{(m)}\equiv W_m(\alpha,\alpha,\gamma)$, and $W_{\mathrm{AF}}^{(m)}\equiv W_m(\alpha,\beta,\gamma)$; where $(\alpha,\beta,\gamma=1,2,\ldots,q)$ and $\alpha\neq\beta\neq\gamma$, $\alpha\neq\gamma$. A similar notation W'_l ($l=\mathrm{F}$, I, and AF) is used for the b' cell, where the superscript has been suppressed since $m=1$ for this cell. Eliminating D from Eq. (3), we obtain that

$$\frac{W_{\mathrm{F}}^{(m)}}{W_{\mathrm{AF}}^{(m)}}=\frac{W'_{\mathrm{F}}}{W'_{\mathrm{Af}}} , \tag{6}$$

$$\frac{W_{\mathrm{I}}^{(m)}}{W_{\mathrm{AF}}^{(m)}}=\frac{W'_{\mathrm{I}}}{W'_{\mathrm{AF}}} . \tag{7}$$

Therefore, our RG preserves the ratios $p_{\mathrm{F}}/p_{\mathrm{AF}}$ and $p_{\mathrm{I}}/p_{\mathrm{AF}}$ of the above probabilities. Since the m sheets are connected only at the roots, the "constrained" partition functions factorize trivially as

$$W_m(\alpha,\beta,\gamma)=[W_1(\alpha,\beta,\gamma)]^m . \tag{8}$$

For the Ising case ($q=2$) obviously only $W_{\mathrm{F}}^{(m)}$ and $W_{\mathrm{I}}^{(m)}$ are defined, and the RG equation (with $K_3=0$) is given by

$$\frac{W_{\mathrm{F}}^{(m)}}{W_{\mathrm{I}}^{(m)}}=\frac{W'_{\mathrm{F}}}{W'_{\mathrm{I}}} \qquad (q=2) . \tag{9}$$

In this case, the K_2 parameter space is closed by renormalization (i.e., if $K_3=0$ then $K'_3=0$ for the triangular cell types considered here).

Notice that Eq. (9) is equivalent to the preservation of the correlation function between any pair of the rooted spins of the $(m\mathrm{SG})_b$, namely,

$$\frac{W_{\mathrm{F}}^{(m)}}{W_{\mathrm{I}}^{(m)}}=\frac{W'_{\mathrm{F}}}{W'_{\mathrm{I}}}\Longleftrightarrow\Gamma_{ij}^{(1)}(G^{(1)},K_2)=\Gamma_{ij}^{(0)}(G^{(0)},K'_2) \qquad (i,j=A,B,C) , \tag{10}$$

where $\Gamma_{ij}^{(1)}(G^{(1)},K_2)$ and $\Gamma_{ij}^{(0)}(G^{(0)},K'_2)$ denote the correlation functions between any two rooted spins at the respective stages $n=1$ and 0 [see Fig. 1(a)] with NN coupling constants K_2 and K'_2 respectively.

Equation (10) follows from the isotropic case ($\Gamma_{AB}=\Gamma_{AC}=\Gamma_{BC}$) of the following relations [which are easily derivable from Eqs. (4) and (5)]:

$$W_{\mathrm{F}}^{(m)}=W_m(1,1,1)=\frac{Z}{8}[\Gamma_{AB}+\Gamma_{AC}+\Gamma_{BC}+1] , \tag{11}$$

$$W_{\mathrm{I}}^{(m)}=W_m(1,1,-1)=\frac{Z}{8}[\Gamma_{AB}-\Gamma_{AC}-\Gamma_{BC}+1] , \tag{12}$$

where

$$\Gamma_{ij} \equiv \langle \alpha_i \alpha_j \rangle \quad (\alpha_i, \alpha_j = \pm 1;\ i,j = A,B,C) \ . \tag{13}$$

IV. A CRITERION FOR THE CHOICE OF CELLS IN AN AF SPIN MODEL

It is well known that the choice of cells in a cell-to-cell RSRG is an important factor for the reliability of its results. One should choose cells that reproduce the geometrical properties of the whole lattices as well as the symmetries of the ground-state configurations of the ordered phases. Although this condition has been taken into account in most RSRG calculations of spin models on Bravais lattices (see, for example, Ref. 49 and references therein), this has been neglected [9,11,12,29,30] in the case of antiferromagnetic models defined on HL. As we will see below, when the symmetries of the ground state are not preserved under renormalization, the RG generates unphysical disconnected basins of attraction. In this section, we propose a criterion for a suitable choice of cells which prevents this kind of problem. First we shall consider the one-parameter RG described by Eq. (9) and derive such a criterion for either Ising antiferromagnets defined on (or approximated by) three-rooted HL or AF Potts model on two-rooted ones. Afterwards we formulate a general criterion which we expect to be valid for AF classical spin models defined on (or approximated by) HL with an arbitrary number of roots.

Although Eq. (9) was mentioned in the context of the AF Ising model on the $(m\mathrm{SG})_b$, this equation is valid for systems described by a one-parameter Hamiltonian defined on cells which have only two different constrained partition functions. Let us, thus, consider the q-state Potts model on two-rooted graphs (or the Ising model on three-rooted ones) with only two-spin interactions, i.e., $K_3 = 0$. The constrained partition functions can be written, for the nonrenormalized cell, as

$$W_l(X) = \sum_{i=0}^{N_b} g_l^{(i)} X^i \quad (l = \mathrm{F,I}) \quad (X \equiv e^{K_2}) \ , \tag{14}$$

where N_b is the number of bonds of the cell and $g_l^{(i)}$ is the degeneracy of the state with energy $\beta\varepsilon_i = -K_2 i$.

Obviously, the first nonzero term $(g_l^{(j_l)} X^{j_l})$ of the lowest order in X^i of Eq. (14) represents the dominant term of W_l for the antiferromagnetic case ($J_2 < 0$) at $T = 0$. We shall denote each such term simply by

$$g_{\mathrm{F}}^{(j_{\mathrm{F}})} X^{j_{\mathrm{F}}} \equiv g_{\mathrm{F}} e^{-\beta\varepsilon_{\mathrm{F}}} \ ,$$

$$g_{\mathrm{I}}^{(j_{\mathrm{I}})} X^{j_{\mathrm{I}}} \equiv g_{\mathrm{I}} e^{-\beta\varepsilon_{\mathrm{I}}} \ ,$$

where ε_{F} (ε_{I}) is the lowest-energy configuration of the AF Potts model on the nonrenormalized cell with the restriction that the spins on the roots are all (are not all) in the same state. Therefore, ε_{F} (ε_{I}) refers to the configuration F (I) where neighbor spins are in different states and (i) either $\sigma_A = \sigma_B$ ($\sigma_A \neq \sigma_B$) in the case of two-rooted cells, or (ii) $\sigma_A = \sigma_B = \sigma_C$ ($\sigma_A = \sigma_B \neq \sigma_C$) in the case of three-rooted ones. ε_{F} and ε_{I} constitute the two lowest energies of the energy spectrum associated with the considered cell and, therefore, the smaller of the two is the ground-state energy for the cell. When $\varepsilon_{\mathrm{F}} < \varepsilon_{\mathrm{I}}$ ($\varepsilon_{\mathrm{F}} > \varepsilon_{\mathrm{I}}$), we shall say that the ground state of the cell is of type F (type I). When $\varepsilon_{\mathrm{F}} = \varepsilon_{\mathrm{I}}$, the type of the ground state is given by the one with higher degeneracy.

Notice that $W_{\mathrm{F}}(X)/W_{\mathrm{I}}(X)$ satisfies the following properties:

$$\frac{W_{\mathrm{F}}(1)}{W_{\mathrm{I}}(1)} = 1 \tag{15}$$

and

$$\lim_{X \to \infty} \frac{W_{\mathrm{F}}(X)}{W_{\mathrm{I}}(X)} \to \infty \ . \tag{16}$$

So we can rewrite Eq. (9) as

$$\frac{g_{\mathrm{F}} e^{-\beta\varepsilon_{\mathrm{F}}} [1 + f_{\mathrm{F}}(X)]}{g_{\mathrm{I}} e^{-\beta\varepsilon_{\mathrm{I}}} [1 + f_{\mathrm{I}}(X)]} = A(X') \tag{17}$$

with

$$A(X') = \frac{g'_{\mathrm{F}} e^{-\beta\varepsilon'_{\mathrm{F}}} [1 + f'_{\mathrm{F}}(X')]}{g'_{\mathrm{I}} e^{-\beta\varepsilon'_{\mathrm{F}}} [1 + f'_{\mathrm{I}}(X')]} \ , \tag{18}$$

where the prime refers to the renormalized b' cell. We have suppressed the superscript (m) since we are now considering systems which, in general, differ from the $(m\mathrm{SG})_b$ fractal.

The function $f_l(X)$ ($l = \mathrm{F,I}$) [and similarly $f'_l(X')$] defined by

$$f_l(X) = \sum_{i > j_l}^{N_b} \frac{g_l^{(i)}}{g_l^{(j_l)}} X^{(i - j_l)} \quad (l = \mathrm{F,I}) \tag{19}$$

is a monotonously increasing function with the following properties:

$$f_l(0) = 0 \tag{20}$$

and

$$\lim_{X \to \infty} f_l(X) = \infty \ . \tag{21}$$

Let us now analyze Eq. (17) in the $X = 0$ limit [i.e., $T \to 0$ in the antiferromagnetic ($J_2 < 0$) case]. Using the general properties of $f_l(X)$ ($l = \mathrm{F,I}$) [Eqs. (20) and (21)] and relations (15) and (16), we obtain (see Table I) the possible solutions of Eq. (17) in this limit for different relationships between ε_{F}, ε_{I} and $\varepsilon'_{\mathrm{F}}$, $\varepsilon'_{\mathrm{I}}$. Three main situations arise from an analysis of this table.

(1) $\varepsilon_{\mathrm{F}} < \varepsilon_{\mathrm{I}}$ and $\varepsilon'_{\mathrm{F}} > \varepsilon'_{\mathrm{I}}$ (case B1). In this case the point $X = 0$ ($K_2 \to -\infty$) is renormalized into $X' \to \infty$ ($K'_2 \to \infty$). Since $K_2^* \to \infty$ is the attractor of the ferromagnetic phase, we conclude that the RG transformation leads to a ferromagnetic solution for the AF case at $T = 0$. This situation arises, for example, in the Ising model on bond HL with even chemical distance b [such as the linear chain, diamond HL (see Fig. 1 of Ref. 13), Wheatstone-bridge HL (see Fig. 2 of 13)] where we renormalize a b cell into a single bond ($b' = 1$). Their typical flow and

TABLE I. Real solutions of Eq. (17) in the $X=0$ limit for different relations among ε_F, ε_I, ε'_F, and ε'_I. Whenever there is the possibility of having two solutions, we indicate them by X'_1 and X'_2.

Possible cases	Solutions of Eq. (17) in the $X=0$ limit $\varepsilon'_F>\varepsilon'_I$	$\varepsilon'_F<\varepsilon'_I$	$\varepsilon'_F=\varepsilon'_I$
Case (A) $\varepsilon_F>\varepsilon_I$ $A(X')=0$	Case (A1) $X'\to 0$	Case (A2) No real solution	Case (A3) No real solution
Case (B) $\varepsilon_F<\varepsilon_I$ $A(X')\to\infty$	Case (B1) $X'\to\infty$	Case (B2) $X'_1\to 0$ and $X'_2\to\infty$	Case (B3) $X'\to\infty$
Case (C) $\varepsilon_F=\varepsilon_I$ $A(X')=\frac{g_F}{g_I}$	Case (C1) $X'\neq 0$ and finite	Case (C2) $X'\neq 0$ and finite	Case (C3) $X'_1\neq 0$ and finite $X'_2\to 0$ if $\frac{g_F}{g_I}=\frac{g'_F}{g'_I}$

phase diagrams in the transmissivity variable[48] $t\equiv\tanh(K_2/2)$ are shown in Fig. 2. Notice that, when the basin of attraction of the ferromagnetic phase contains more than one point [Fig. 2(b)], this choice of cells generates an unphysical disconnected ferromagnetic phase.

(2) The inequality between ε_F and ε_I is preserved under renormalization (cases A1 and B2). For these cases, $X'=0$ is a solution of Eq. (17) for $X=0$, which means that the RG transformation presents an antiferromagnetic solution, at least, for $T=0$. This situation can be found, for example, in the Ising model on bond HL with odd chemical distance such as the linear chain, Migdal-Kadanoff-type HL [see Figs. 1(a)–1(f) of Ref. 30] and also on bond HL with even chemical distances where we renormalize a b cell into a b' one with $b'=b/2\neq 1$. In Fig. 3, we plotted the two branches $t'_+(t)$ and $t'_-(t)$ of the renormalized transmissivity $[t'_+(t)\geq 0$ and $t'_-(t)\leq 0]$ which appear in the latter case for $b=4$ and $b'=2$ in the Ising model on the linear chain [Fig. 3(a)], and on the diamond HL [Fig. 3(b)]. The union of $t'_+(t)$ (which is equal to the solution obtained for the renormalization of the $b=2$ cell into a bond) for $0\leq t\leq 1$ with $t'_-(t)$ for $-1\leq t\leq 0$ provides a solution [which we denote by $t'_{ph}(t)$] which is physically meaningful. On the linear chain this solution leads to the exact known phase diagram, while on the diamond HL it yields to the expected antiferromagnetic order at zero temperature for the Ising model with $J_2<0$ (notice that in this case there is no frustration in the thermodynamic limit). Concerning the Ising model on HL with odd chemical distances, the solutions $t'(t)$ obtained for $b'=1$ are qualitatively similar to $t'_{ph}(t)$, not requiring, therefore, the use of bigger cells. Differently from situation (1), we note that points with $K_2<0$ $(-1<t<0)$ are renormalized into $K'_2<0$, causing

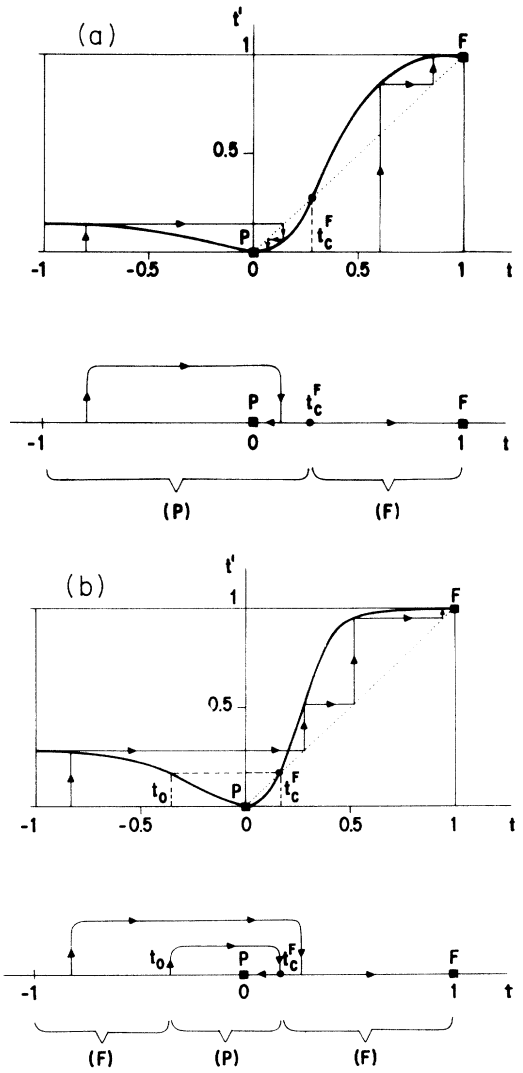

FIG. 2. The RG transformation on the t variable and the respective flow diagram for (a) the linear chain, renormalization $b=2\to b'=1$; (b) the diamond HL, renormalization $b=2\to b'=1$. ● and ■ represent, respectively, the unstable and the fully stable fixed points. The dotted line denotes the $t'=t$ curve and the arrows indicate the RG flow directions. By successive iterations, an initial value $t\neq 1$ (P phase) in (a) will converge to the paramagnetic (P) attractor $t_P^*=0$. In (b), an initial value $t<t_0$ or $t>t_c^F$ will converge to the ferromagnetic attractor $t_F^*=1$. Another initial value $t_0<t<t_c^F$ (P phase) will converge to the $t_P^*=0$.

no disconnectedness in the basins of attraction of the phases.

(3) $\varepsilon_F=\varepsilon_I$ (cases C1, C2, and C3). In this situation the RG transformation provides a finite and non-null solution for X'. Furthermore, a solution $X'<1$ can appear when the type of the ground state is preserved under renormalization. On the other hand, when there is no such preservation we do not know any example in which $X'<1$ is a solution. When $X'>1$, the behavior is qualitatively similar to situation (1): any $K_2<0$ renormalizes after one RG step to $K'_2>0$. One example of this situa-

tion will be given in Sec. V A (AF Ising model on the $(mSG)_2$ for $b=2$ and $b'=1$]. When $X'<1$ two possibilities can happen:

(3a) Successive iterations of any $K_2'<0$ converge to the paramagnetic attractor $t_P^*=0$ through negative values of K_2 [Fig. 4(a)]. Such behavior occurs, for instance, in the AF Ising model on the $(2SG)_2$ for $b=4$ and $b'=2$ (see Sec. V A).

(3b) If $|K_2'|$ is large enough, it can lead to an antiferro-

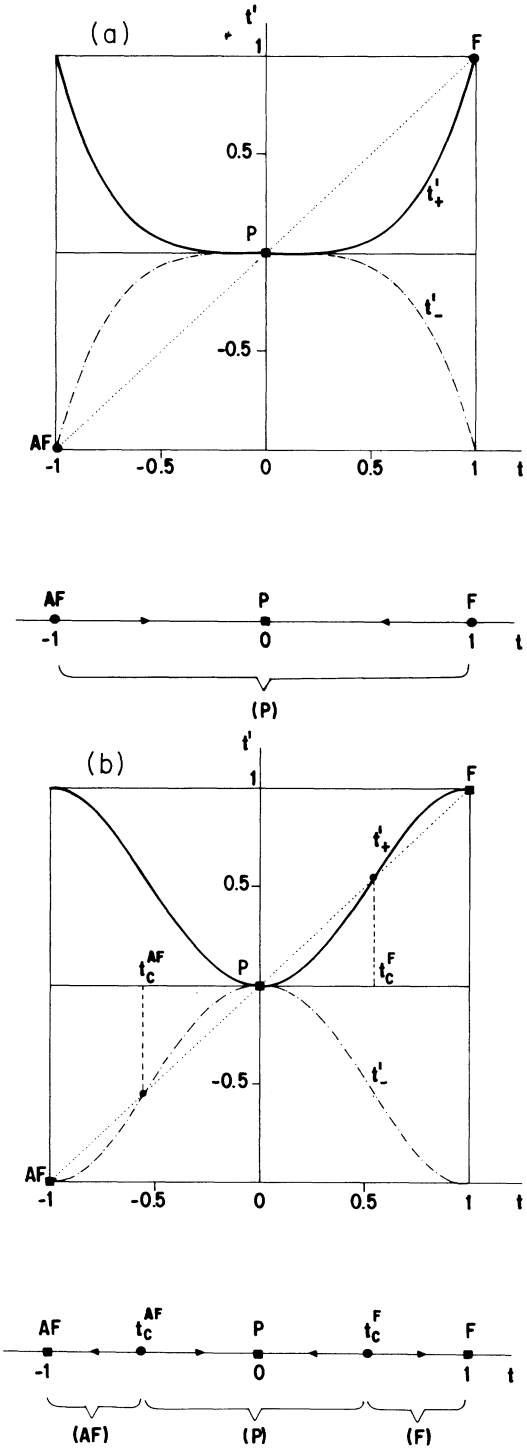

FIG. 3. The RG transformation $t'(t)$ and the respective phase diagram for (a) the linear chain, renormalization $b=4\rightarrow b'=2$; (b) diamond HL, renormalization $b=4\rightarrow b'=2$. The solid and dash-dotted lines represent, respectively, the positive $[t'_+(t)]$ and negative $[t'_-(t)]$ solutions.

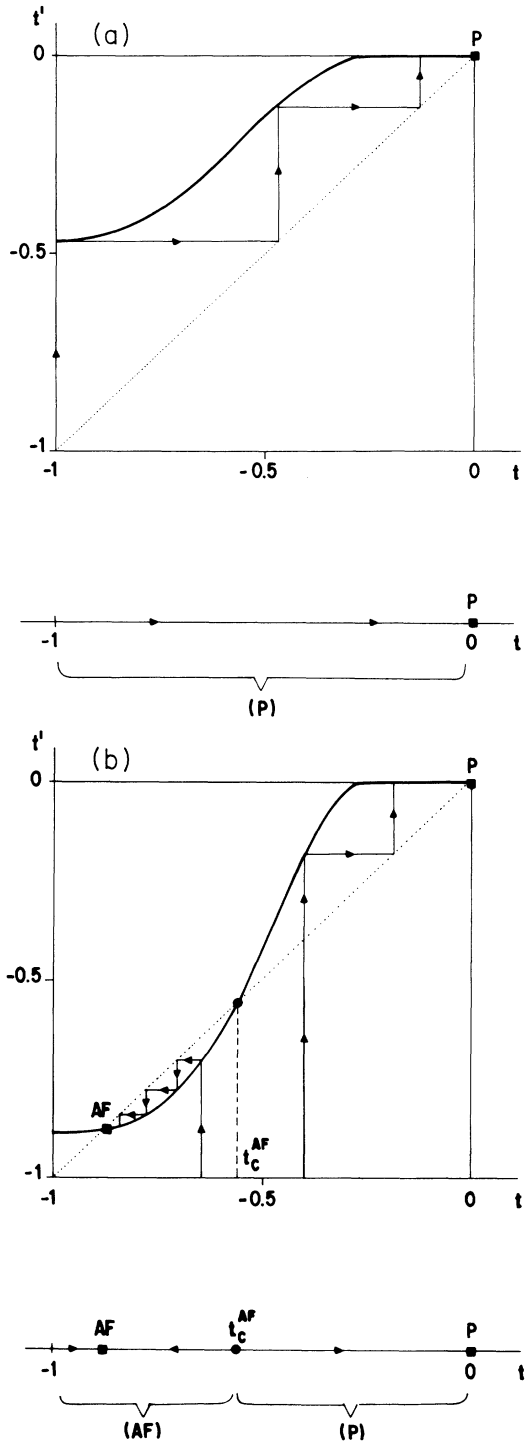

FIG. 4. Typical plot of a RG transformation $t'(t)$ for negative values of t and the respective phase diagram for situation (3) ($\varepsilon_F=\varepsilon_I$). (a) The finite solution, $K_2'<0$, at $T=0$ converges after successive iterations to the paramagnetic attractor (t_P^*), (b) when $|K_2'|$ is large enough it leads to a finite-temperature antiferromagnetic (AF) attractor.

magnetic attractor at a finite temperature, i.e., $t^{*}_{AF} \neq -1$ as illustrated in Fig. 4(b). We will see one example of this situation in the AF Ising model on the $(m\mathrm{SG})_4$ for $m \geq 116$ (see Sec. V B 1). Using a rescaling argument, Berker and Kadanoff[34] showed how this behavior can arise, in the RSRG scheme, on systems whose residual entropy per particle is nonzero, such as the antiferromagnetic q-state Potts model on hypercubic lattices,[34] on Migdal-Kadanoff-type HL,[30] on Sierpinski carpet,[6,47] and on Sierpinski pastry shell;[6] they also suggested that this unusual phase is characterized by a power-law decay of correlations.

We conclude from the above analysis that, when $\varepsilon_F \neq \varepsilon_I$ and $\varepsilon'_F \neq \varepsilon'_I$, one should choose cells whose ground states are from the same type, otherwise unphysical disconnected phases can appear. When $\varepsilon_F = \varepsilon_I$ [which is the case of the Ising model on all the fractal families $(m\mathrm{SG})_b$], we showed that $K_2 \to -\infty$ is not a fixed point, or, in other words, the zero-temperature character of the antiferromagnet is not preserved under RG, since the rooted spins after renormalization become nearest neighbors and have a nonzero probability of being all in the same state. In the latter case, if there is preservation of the type of the cellular ground state, then an unusual phase characterized by an attractor at a non-null temperature can appear.

We also verified in some examples of a two-parameter RG (see, for example, Secs. V B 2 and V B 3) that a necessary (but not sufficient) condition for obtaining reliable results is to choose cells which preserve the type of the ground state under renormalization. In fact, we believe that this criterion can be generalized to an n-parameter $RG(n>1)$ for AF classical spin models defined on (or approximated by) HL with many roots and such that there are $(n+1)$ different restricted partitions functions. The RG recursive relations are, then, constructed by preserving n different ratios of these restricted partition functions. In this case there will be $(n+1)$ configurations (with respective energies $\varepsilon_1, \varepsilon_2, \ldots, \varepsilon_{n+1}$ and degeneracies $g_1, g_2, \ldots, g_{n+1}$) where the rooted spins are at frozen states and the remaining spins are such that two nearest neighbors are at different states. If ε_i is the smallest energy (or in the case of equalities among the energies, if g_i is the biggest degeneracy), then we say that the ground state of the cell is of type i. The generalization of the above criterion would then be the following: *A necessary but not sufficient condition for the above n-parameter RG to describe well AF classical spin models defined on (or approximated by) multirooted HL is to use cells that preserve the type of the ground state under renormalization.*

V. RESULTS

In this section we consider the Ising model on the $(m\mathrm{SG})_2$ and the $q=2$-, 3-, and 4-state Potts model on the $(m\mathrm{SG})_4$ family.

A. Ising model on the $(m\mathrm{SG})_2$

In this case, renormalizing the $b=2$ cell with m sheets [Fig. 1(a), $n=1$] into the $b'=1$ cell with one sheet [Fig. 1(a), $n=0$], Eq. (17) becomes

$$\left[\frac{4X^3[1+f_F(X)]}{3X^3[1+f_I(X)]}\right]^m = \frac{X'^3}{X'} = X'^2 \tag{22}$$

with

$$f_F(X) = \tfrac{3}{4}X^2 + \tfrac{1}{4}X^6 \tag{23}$$

and

$$F_I(X) = \tfrac{4}{3}X^2 + \tfrac{1}{3}X^4 , \tag{24}$$

which agrees, for $m=1$, with Eq. (1) of Ref. 1.

Rewriting Eq. (22) in terms of the finite-valued $t \equiv \tanh(K_2/2)$ variable, we obtained $t'(t)$ and the corresponding phase diagram shown in Fig. 5. The exact ferromagnetic critical temperature $K_B T_c^F / J_2$ is plotted as a function of m in Fig. 6. It should be noted that, for $m=2$, points with $-1 \leq t < 0$ converge to the paramag-

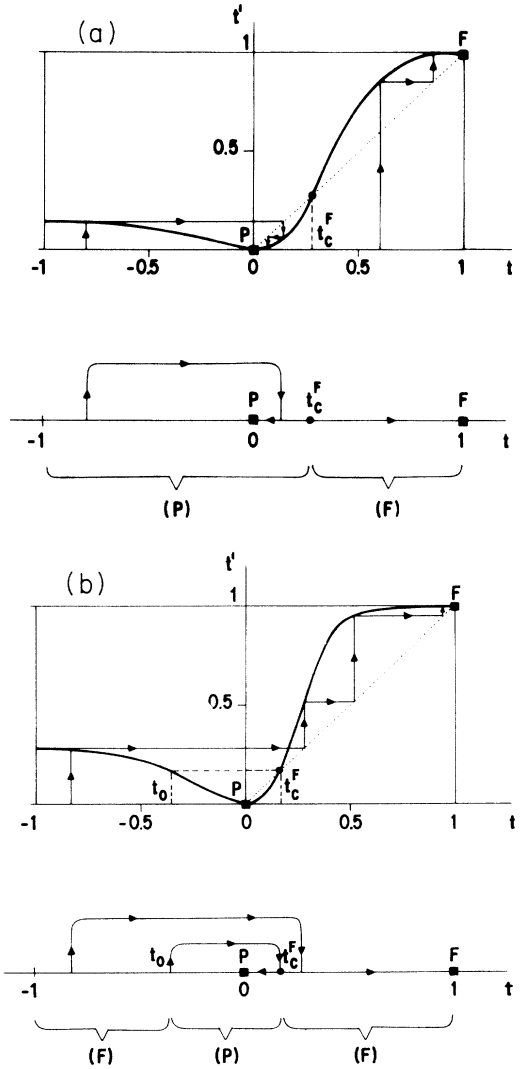

FIG. 5. The RG transformation [Eq. (22)] and the respective phase diagram for the Ising model on the $(m\mathrm{SG})_2$; renormalization $b=2 \to b'=1$. (a) $m=2$, (b) $m=3$; the flow diagrams for $m>3$ are qualitatively similar.

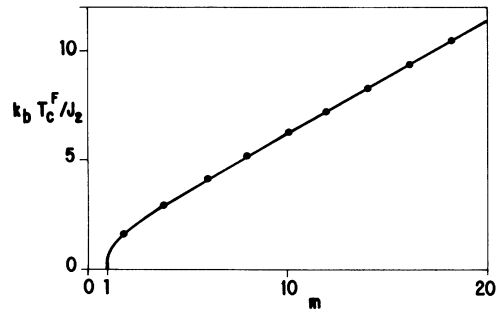

FIG. 6. The exact P-F critical temperature as a function of m for the Ising model on the $(m\mathrm{SG})_2$: renormalization $b=2\rightarrow b'=1$.

netic attractor through positive (instead of negative) values of K_2'. Moreover, for $m\geq 3$, points with $-1\leq t<t_0$ $[t'(t_0)=t_c^{\mathrm{F}}]$ converge to the ferromagnetic attractor, generating, thus, a disconnected unphysical ferromagnetic phase. This behavior can be understood in terms of the analysis of the energies $(\varepsilon_{\mathrm{F}},\varepsilon_{\mathrm{I}})$ and degeneracies $(g_{\mathrm{F}},g_{\mathrm{I}})$ introduced in the previous section given by

$$\varepsilon_{\mathrm{F}}=-3J_2m,\quad g_{\mathrm{F}}=4^m,\quad \varepsilon_{\mathrm{F}}'=-3J_2',\quad g_{\mathrm{F}}'=1\ ,$$

$$\varepsilon_{\mathrm{I}}=-3J_2m,\quad g_{\mathrm{I}}=3^m,\quad \varepsilon_{\mathrm{I}}'=-J_2',\quad g_{\mathrm{I}}'=1\ .$$

So, the ground state for the antiferromagnetic case of this model on the nonrenormalized cell ($b=2$, m sheets) is of *type F* (because, in spite of $\varepsilon_{\mathrm{F}}=\varepsilon_{\mathrm{I}}$, $g_{\mathrm{F}}>g_{\mathrm{I}}$) while it is of *type I* on the renormalized one ($b'=1$) (because $\varepsilon_{\mathrm{I}}'<\varepsilon_{\mathrm{F}}'$). In order to avoid the unphysical behavior above caused by the lack of preservation of the type of the ground state, we should choose other cells that reproduce exactly the same fractal, for instance, $b=4$ with m sheets [see Fig. 1(a), $n=2$] and the renormalized cell $b'=2$ with m sheets [see Fig. 1(a), $n=1$].

The RG transformation [Eq. (17)] becomes, with this new choice of cells,

$$\frac{g_{\mathrm{F}}(m)X^{9m}[1+f_{\mathrm{F}}^{(m)}(X)]}{g_{\mathrm{I}}(m)X^{9m}[1+f_{\mathrm{I}}^{(m)}(X)]}=\frac{4X'^3[1+f_{\mathrm{F}}'(X')]}{3X'^3[1+f_{\mathrm{I}}'(X')]}\ , \tag{25}$$

where the dependence on m of the $g_{\mathrm{F}}(m)$ and $g_{\mathrm{I}}(m)$ are not powers any more of $g_{\mathrm{F}}(1)$ and $g_{\mathrm{I}}(1)$, for example, $g_{\mathrm{F}}(1)=280$, $g_{\mathrm{I}}(1)=273$, $g_{\mathrm{F}}(2)=10\,900$, $g_{\mathrm{I}}(2)=9675$, $g_{\mathrm{F}}(3)=480\,844$, $g_{\mathrm{I}}(3)=356\,265$. $f_{\mathrm{F}}^{(m)}$ and $f_{\mathrm{I}}^{(m)}$ are smooth polynomials of respective degrees $18m$ and $16m$, $f_{\mathrm{F}}'(X')$ and $f_{\mathrm{I}}'(X')$ have the same functional forms as those of Eqs. (23) and (24), respectively. It should be noted that, for any value of m, the ground state for the AF case of this model is of *type F* for both cells since, in spite of $\varepsilon_{\mathrm{F}}=\varepsilon_{\mathrm{I}}=-9J_2m$ and $\varepsilon_{\mathrm{F}}'=\varepsilon_{\mathrm{I}}'=-3J_2'm$, $g_{\mathrm{F}}(m)>g_{\mathrm{I}}(m)$ for all m and $g_{\mathrm{F}}'>g_{\mathrm{I}}'$. On the other hand, one can easily show that Eq. (25) presents solutions with $X'<1$ at $X=0$ only for $g_{\mathrm{F}}(m)/g_i(m)<\frac{4}{3}$. As we can see from the above degeneracies, this condition holds exclusively for $m=1$ and 2. In Fig. 7, it is plotted, for $m=2$, the real solutions on the t variable which can have any physical meaning. The positive solution $t'_+(t)$ is exactly the one obtained in the previous renormalization ($b=2\rightarrow b'=1$). Similar to

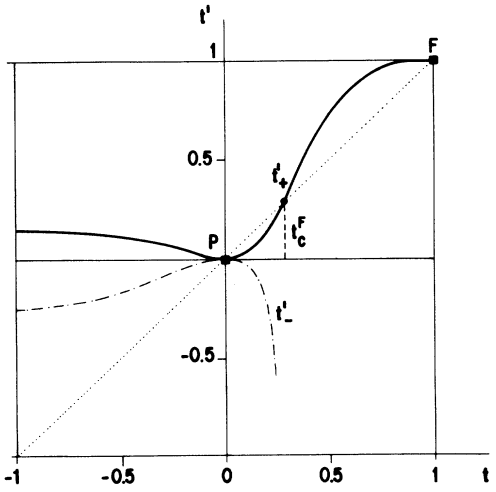

FIG. 7. Solutions of the RG transformation [Eq. (25)] for the Ising model on the $(2\mathrm{SG})_2$: renormalization $b=4\rightarrow b'=2$. The solid and dash-dotted lines denote, respectively, the positive and negative branches.

the examples of case (2) of Sec. IV, the physical solution is obtained by the union of $t'_+(t)$ for $0\leq t\leq 1$ with the negative one t'_- for $-1\leq t\leq 0$. Similar to the Ising antiferromagnet on the triangular lattice which, due to its full frustration, is paramagnetic even at $T=0$,[33] there is no AF order (not even at $T=0$) for this model on the fully frustrated fractal $(2\mathrm{SG})_2$. For $m\geq 3$ the negative branch becomes complex near $t=-1$ and, therefore, $t'(t)$ is given by the positive branch $t'_+(t)$ which generates a disconnected ferromagnetic phase. Despite the preservation, for $m>3$, of the type of cellular ground state, the considered RG leads to unphysical results—this example illustrates the insufficiency of the criterion stated in Sec. IV. We believe that, for a given $m\geq 3$, the convenient choice of cells which leads to the exact results for the AF Ising model on the $(m\mathrm{SG})_2$ should have sides $b=2^n$ and $b'=2^{n-1}$, where $n(m)$ is such that each basin of attraction of a phase is connected.

B. Potts model on the $(m\mathrm{SG})_4$

Let us consider now the $q=2$-, 3-, and 4-state Potts model on a different fractal family, namely, on the $(m\mathrm{SG})_4$. In this case, we renormalize the $b=4$ cell with m sheets [see Fig. 1(c)] into the $b'=1$ cell with one sheet [see Fig. 1(a), $n=0$].

1. $q=2$ case (Ising model)

In this case the RG transformation [Eq. (17)] is written as

$$\frac{(168)^mX^{10m}[1+f_{\mathrm{F}}(q=2,X)]^m}{(175)^mX^{10m}[1+f_{\mathrm{I}}(q=2,X)]^m}=\frac{X'^3}{X'}\ , \tag{26}$$

where

$$f_F(q=2,X)=\tfrac{1}{168}[847X^2+1200X^4+975X^6+595X^8 +213X^{10}+75X^{12}+13X^{14} +9X^{16}+X^{20}] \quad (27)$$

and

$$f_I(q=2,X)=\tfrac{1}{175}[812X^2+1243X^4+991X^6+545X^8 +223X^{10}+81X^{12}+21X^{14} +4X^{16}+X^{18}] . \quad (28)$$

Notice that the above expressions lead, for $m=1$ and

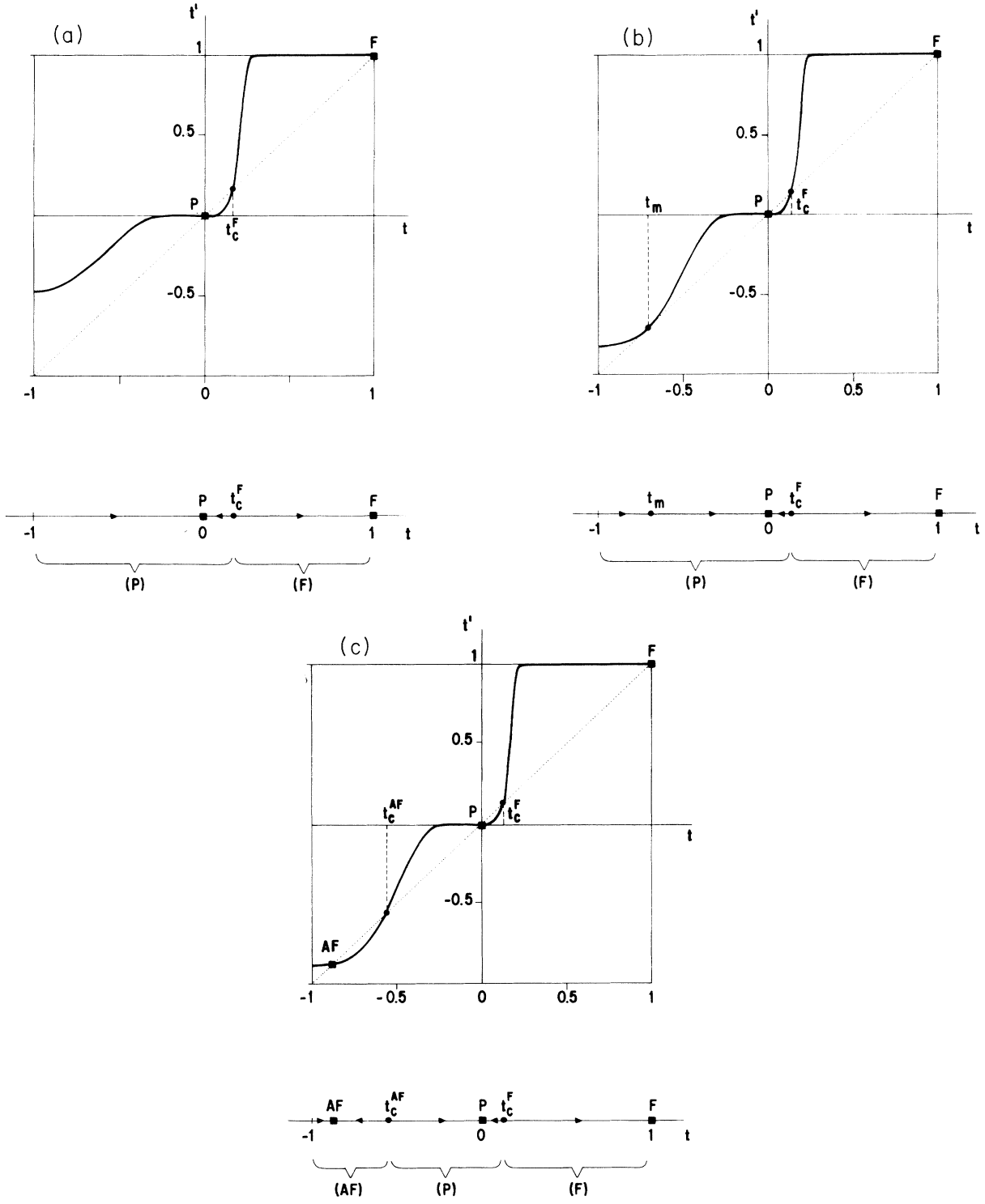

FIG. 8. The RG transformation [Eq. (26)] and the respective phase diagram for $q=2$ on the $(m\mathrm{SG})_4$ for different values of m: (a) $m=50$ (typical of $m<m_c$), (b) $m=m_c\cong 115.57$, (c) $m=140$ (typical of $m>m_c$). t_m is a marginal fixed point.

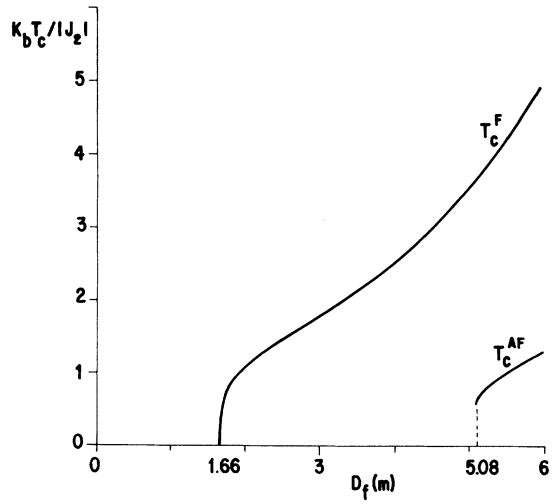

FIG. 9. Critical temperatures of the para-ferromagnetic (T_c^F) and para-antiferromagnetic (T_c^{AF}) transitions of the Ising model on the $(m\mathrm{SG})_4$. Notice the jump discontinuity of $K_B T_c^{AF}/|J_2|$ at $D_f^c=5.08$.

$K \gg 1$, to

$$e^{-2K'} \cong e^{-2K}+4e^{-4K}+O(e^{-6K}) ,$$

which agrees with Eq. (9) of Ref. 9 valid for all b and $m=1$. In Fig. 8 is shown the plot of Eq. (26) on the t variable and the respective phase diagrams for different values of m.

It should be noted that this is an example of the case (C1) of Table I where the ground state for the AF case of this model is of type I on both $b=4$ and $b'=1$ cells and where the suitable negative solution for negative values of K_2 ($-1<t<0$) appears. We want to stress that a new negative solution for $-1<t<0$ does not appear when we increase the sizes of the cells to $b=16$ and $b'=4$ since, for any fixed value of $W'_F/W'_I|_{b'=4}$ there corresponds a *unique* value of t' where $-1 \le t' \le 0$. This is an indication that our solution might be the *exact* one.

From Fig. 8 we see that an unusual AF phase appears only for $m > m_c \cong 115.57$ ($D_f^c \cong 5.1$). This occurs only when, for $T=0$, the probability $p_I(m)$ of the configuration (I) of the nonrenormalized cell becomes much bigger than the probability $p_F(m)$ of the configuration (F) $[p_I(m_c)/p_F(m_c) \cong 112]$. We obtained, for $J_2<0$, the same RG behavior with increasing D_f as the one proposed by Berker and Kadanoff[34] for d-dimensional systems with residual entropy per site with increasing d. In Fig. 9 the para-ferromagnetic and para-antiferromagnetic critical temperatures for this case are shown.

Let us now calculate the correlation function Γ_{AB} on the $(m\mathrm{SG})_4$ for a fixed $m > m_c$ along the unusual phase with attractor $X^*_{AF} \neq 0$. Using the X variable ($X \equiv e^{K_2}$) and iterating n times Eq. (10), we obtain that

$$\Gamma^{(n)}_{AB}(G^{(n)},X)=\Gamma^{(0)}_{AB}[G^{(0)},X^{(n)}=(T_m)^n] , \tag{29}$$

where

$$X'=T_m(X) . \tag{30}$$

$T_m(X)$ is given explicitly by the square root of the left-hand side of Eq. (26). $G^{(n)}$ is the nth stage of the $(m\mathrm{SG})_4$ and $X^{(n)}$ is the coupling constant obtained after n iterations of the recursive equation (30).

Through linerization of T_m around the AF attractor fixed point, X^*_{AF}, we obtain

$$X^{(1)}-X^*_{AF}=\lambda_m(X-X^*_{AF})+0(X^2) , \tag{31}$$

where

$$\lambda_m=(\partial T_m/\partial X)|_{X=X^*_{AF}}<1 . \tag{32}$$

Iterating Eq. (31) n times leads to

$$X^{(n)}-X^*_{AF} \cong (\lambda_m)^n(X-X^*_{AF}) . \tag{33}$$

Combining Eqs. (29) and (33) with the expression of $\Gamma^{(0)}_{AB}(G^{(0)},X)$ given by

$$\Gamma^{(0)}_{AB}(G^{(0)},X)=2\frac{(X^2+1)}{X^2+3}-1 , \tag{34}$$

we finally arrive, in the fractal limit ($n \to \infty$), at

$$\Gamma_{AB}(G,X) \equiv \lim_{n\to\infty}[\Gamma^{(n)}_{AB}(G^{(n)},X)-\Gamma^{(\infty)}_{AB}(G^{(\infty)},X^*_{AF})]$$
$$\cong B_m(X) r_{AB}^{-a(m)} \quad (r_{AB} \to \infty) , \tag{35}$$

where

$$B_m(X)=4\frac{(X^{*2}_{AF}+1)}{(X^{*2}_{AF}+3)}\left[X^*_{Af}\left[\frac{1}{(1+X^{*2}_{AF})}-\frac{1}{(3+X^{*2}_{AF})}\right]\right]$$
$$\times(X-X^*_{AF}) . \tag{36}$$

r_{AB} is the chemical distance between the roots A and B at the nth stage of the $(m\mathrm{SG})_4$ given by

$$r_{AB}=4^n \tag{37}$$

and $a(m)$ is defined as

$$a(m)=-\frac{\ln\lambda_m}{\ln 4} . \tag{38}$$

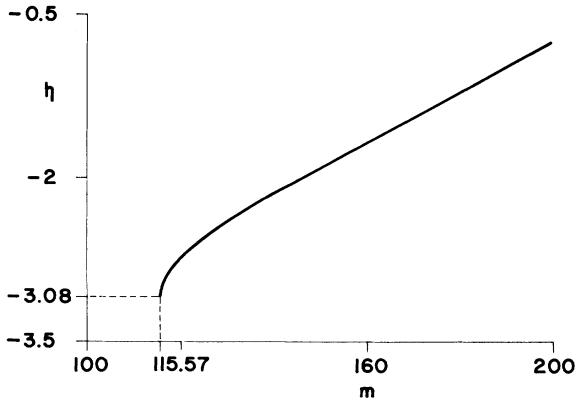

FIG. 10. Critical exponent η vs m along the whole unusual phase of the Ising model on the $(m\mathrm{SG})_4$ for $m > m_c \cong 115.57$.

Equation (35) confirms, thus, the power-law decay of correlations along this whole unusual phase as suggested by Berker and Kadanoff.[34]

Assuming that, similar to the asymptotic behavior of $\Gamma(r\to\infty)$ in d-dimensional Bravais lattices,

$$\Gamma_{AB}(G,X)\cong r_{AB}^{-[D_f(m)-2+\eta_{AF}(m)]} \quad (r_{AB}\to\infty)\ , \tag{39}$$

we obtained the critical exponent η_{AF} as a function of m shown in Fig. 10.

2. 3-state Potts model

For $q=3$, the RG transformation [Eqs. (6) and (7)] can be written as

$$\frac{(24)^m X^{2m}[1+f_F(q=3,X,Y)]^m}{[1+f_{AF}(q=3,X,Y)]^m}=\frac{X'^3Y'}{1}\ , \tag{40}$$

$$\frac{(4)^m X^m[1+f_I(q=3,X,Y)]^m}{[1+f_{AF}(q=3,X,Y)]^m}=\frac{X'}{1}\ , \tag{41}$$

where $f_l(q=3,X,Y)$ (l=F, I, AF) are polynomials in X and Y with many terms whose first and last ones are given by

$$f_F(q=3,X,Y)=\tfrac{1}{24}[204X+\cdots+X^{28}Y^{10}]\ , \tag{42}$$

$$f_I(q=3,X,Y)=\tfrac{1}{4}[28X+\cdots+X^{27}Y^{9}]\ , \tag{43}$$

and

$$f_{AF}(q=3,X,Y)=[48X^2+\cdots+3X^{26}Y^{8}]\ . \tag{44}$$

Using the finite value transmissivity[48] variable t_2 $[-1/(q-1)\le t_2\le 1]$, defined by

$$t_2=\frac{e^{K_2}-1}{e^{K_2}+(q-1)}$$

and a similar variable associated with three-spin interactions:

$$t_3=\frac{e^{K_3}-1}{e^{K_3}+(q-1)}\ ,$$

we obtained the flow and phase diagrams for $m=2$ shown in Fig. 11(a) as well as the critical frontiers for different values of m [see Fig. 11(b)]. Table II contains the semistable fixed points t_c^F and t_c^{AF} which govern the respective critical behaviors of the P-F and P-AF transitions.

It should be noted that the critical frontier P-F (P-AF) is tangent to the axis $t_3=-\frac{1}{2}$ ($t_3=1$) and finishes at the respective attractor F ($K_2\to\infty$, $K_3\to-\infty$) [AF($K_2\to-\infty$, $K_3\to\infty$)]. This unusual behavior, where the attractor is localized on a critical line, was also obtained for the pair of attractors ($K_2\to-\infty$, $K_{NN}\to-\infty$) and ($K_2\to\infty$, $K_{NN}\to-\infty$) in the Ising model with nearest-neighbor (K_2) and next-nearest-neighbor (K_{NN}) interactions on the square lattice.[49] In both cases the attractors are characterized by infinite coupling constants and asymptotic behaviors which depend on the angle of approach.

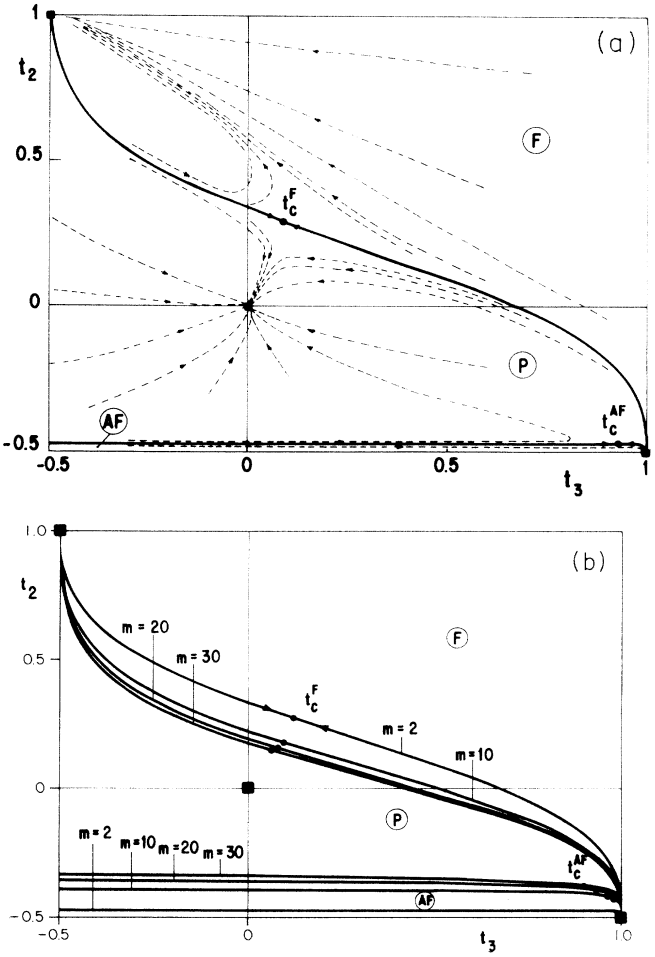

FIG. 11. The 3-state Potts model on the $(m\mathrm{SG})_4$. (a) Flow diagram for $m=2$. ● and ■ denote, respectively, the semistable and fully stable fixed points; the dashed and solid lines indicate the flows and the critical frontiers, respectively. (b) P-F and P-AF critical frontiers for different values of m.

For increasing values of m, the connectivity increases strengthening the correlations; consequently, the regions of the ordered phases become larger as shown in Fig. 11(b). On the other hand, in the $m\to1$ limit, where the order of ramification (R) becomes finite, the critical fron-

TABLE II. Values of the semistable fixed points t_c^F and t_c^{AF}, for $q=3$ on the $(m\mathrm{SG})_4$ for different values of m.

m	$t_c^F\equiv(t_3,t_2)$	$t_c^{AF}\equiv(t_3,t_2)$
1	$(-\frac{1}{2},1)$	$(1,-\frac{1}{2})$
2	(0.070 07, 0.294 70)	(0.934 61, −0.472 41)
3	(0.094 03, 0.243 17)	(0.866 71, −0.450 39)
4	(0.093 06, 0.223 28)	(0.810 11, −0.436 84)
5	(0.087 80, 0.212 34)	(0.760 41, −0.426 83)
10	(0.062 97, 0.189 52)	(0.587 91, −0.395 95)
30	(0.028 23, 0.161 99)	(0.371 36, −0.343 69)
50	(0.017 94, 0.148 94)	(0.311 09, −0.319 09)
70	(0.013 01, 0.140 16)	(0.281 10, −0.303 43)
100	(0.009 09, 0.130 81)	(0.255 66, −0.287 59)

tier P-AF (P-F) reduces to the $t_2=-\frac{1}{2}$ ($t_2=1 \cup t_3=1$) axis bringing the critical temperature down to $T_c=0$ in both cases, and the semistable fixed point t_c^{AF} (t_c^F) coincides with its respective attractor AF (F). This is in agreement with the observed fact (see, for example, Ref. 3) that short-range spin models on structures with finite order of ramification do not present phase transition at finite temperatures. It should be noted that, different from the fully frustrated Ising model on the $(m\mathrm{SG})_4$ for $m \leq m_c$, the 3-state Potts model presents, for all values of m, an antiferromagnetic ordering at $T=0$ with a nonfrustrated ground state. Notice also that, in the AF case, the ground states of the used cells are both of type AF (considering $J_2<0$ and $J_3<-3J_2$) and are nondegenerated. This case is a generalization to two parameters of case (A1) of Table I, where $T=0$ ($X\to 0$, $Y\to\infty$) is a fixed point.

3. 4-state Potts model

For $q=4$, the RG transformation [Eqs. (6) and (7)] is given by

$$\frac{(360)^m[1+f_F(q=4,X,Y)]^m}{(616)^m[1+f_{AF}(q=4,X,Y)]^m}=\frac{X'^3Y'}{1} \tag{45}$$

and

$$\frac{(456)^m[1+f_I(q=4,X,Y)]^m}{(616)^m[1+f_{AF}(q=4,X,Y)]^m}=\frac{X'}{1}\ , \tag{46}$$

where the first and last terms of $f_l(q=4,X,Y)$ are

$$f_F(q=4,X,Y)=\tfrac{1}{360}[8064X+\cdots+X^{30}Y^{10}]\ , \tag{47}$$

$$f_I(q=4,X,Y)=\tfrac{1}{456}[8928X+\cdots+X^{28}Y^{9}]\ , \tag{48}$$

and

$$f_{AF}(q=4,X,Y)=\tfrac{1}{616}[9168X+\cdots+3X^{26}Y^{8}]\ . \tag{49}$$

The AF ground state of this model is of type AF on the nonrenormalized cell (since, in spite of $\varepsilon_{AF}=\varepsilon_I=\varepsilon_F=0$, $g_{AF}>g_I>g_F$) and also on the renormalized one (since $\varepsilon'_{AF}<\varepsilon'_I$ and $\varepsilon'_{AF}<\varepsilon'_F$, considering $J_2<0$ and $J_3<-3J_2$). This is a generalization to two parameters of case (C1) of Table I where, due to the degeneracies g_I and g_F, $T=0$ is not a fixed point for any value of m.

The phase diagram on the (t_2,t_3) variables for $m=2$ and 20 are shown in Fig. 12. Similar to the $q=2$ case, it appears an unusual AF phase with attractor at $T\neq 0$ only for $D_f(m)\geq 3.7$ ($m\geq m_c\cong 17.63$), when the probability $p_{AF}(m)$ of the configuration (AF) of the nonrenormalized cell at $T=0$ becomes much bigger than those of the configurations (I) and (F) [$p_{AF}(m_c)/p_I(m_c)\cong 199$ and $p_{AF}(m_c)/p_F(m_c)\cong 12\,775$]. Table III contains the semistable fixed points t_c^F and t_c^{AF} governing the P-F and P-AF phase transitions, respectively, as well as the attractor t^*_{AF} of the unusual AF phase. Similar to the Ising case, as m tends to m_c, the fixed points t_c^{AF} and t^*_{AF} approach each other until they merge, for $m=m_c$, into a single marginal one where $\nu_T^{AF}\to\infty$. Notice also that, for $m\gg m_c$, the AF attractor converges to $T=0$ since p_I

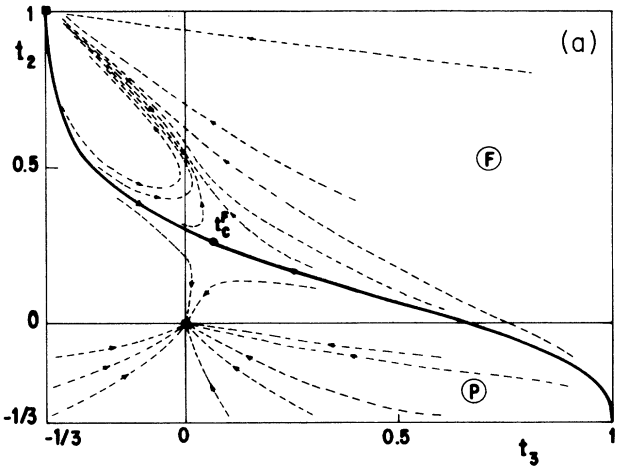

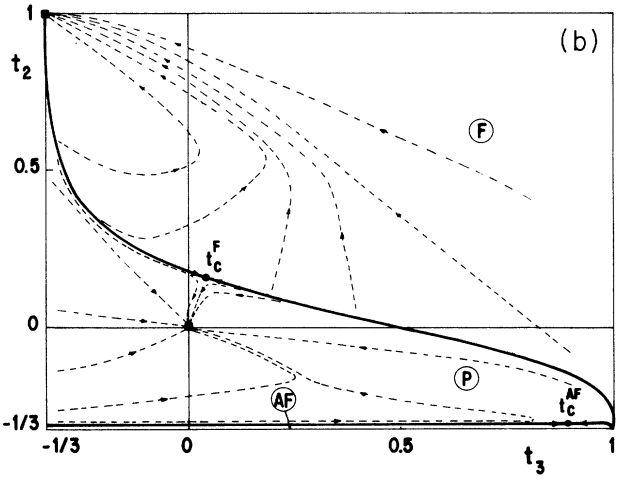

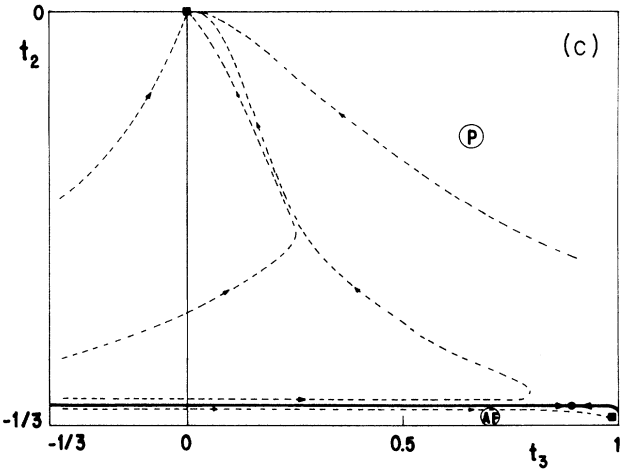

FIG. 12. Flow diagrams for the 4-state Potts model on the $(m\mathrm{SG})_4$. (a) The $m=2$ case, which exhibits only the P and F phases. (b) The $m=20$ case, where the AF phase with attractor at a finite temperature appears, shown on the inset (c). The flow diagrams for other values of m with $m>m_c\cong 17.63$ are qualitatively similar to that of $m=20$.

TABLE III. Values of the semistable fixed points t_c^{F}, t_c^{AF}, and the unusual AF attractor (t_{AF}^*) for $q=4$ on the $(m\mathrm{SG})_4$ for different values of m.

m	$t_c^{\mathrm{F}}\equiv(t_3,t_2)$
1	$(-\frac{1}{3},1)$
2	(0.073 06, 0.252 62)
3	(0.099 57, 0.207 71)
4	(0.100 37, 0.191 44)
5	(0.095 98, 0.183 03)
10	(0.071 43, 0.167 25)
12	(0.064 29, 0.164 20)
14	(0.058 41, 0.161 72)
16	(0.053 49, 0.159 58)
18	(0.049 32, 0.157 69)
20	(0.045 74, 0.155 97)

m	$t_c^{\mathrm{AF}}\equiv(t_3,t_2)$	$t_{\mathrm{AF}}^*\equiv(t_3,t_2)$
$m_c=17.634\,36$	(0.970 21, −0.326 47)	(0.970 21, −0.326 47)
18	(0.946 70, −0.322 70)	(0.985 01, −0.329 27)
20	(0.891 29, −0.315 22)	(0.995 90, −0.331 86)
25	(0.795 87, −0.303 94)	(0.999 52, −0.333 07)
30	(0.724 91, −0.295 80)	(0.999 92, −0.333 27)
35	(0.669 27, −0.289 25)	(0.999 98, −0.333 32)
40	(0.624 44, −0.283 74)	(0.999 99, −0.333 33)
45	(0.587 55, −0.278 98)	(0.999 99, −0.333 33)

and p_{F} become neglectable in comparison with $p_{\mathrm{AF}}[p_{\mathrm{I}}(m=45)/p_{\mathrm{AF}}(m=45)\cong 10^{-6}$ and $p_{\mathrm{F}}(m=45)/p_{\mathrm{AF}}(m=45)\cong 10^{-11}]$. Although the above behavior confirms the one suggested by Berker and Kadanoff,[34] it remains to be proved that the correlations decay algebraically along this entire distinctive phase.

The problem of making out the ordering type (if any) at $T=0$ of the $(q=q_0+1)$-state AF Potts model on a q_0-partite lattice (i.e., which can be split into q_0 sublattices in such a manner that any two sites of one sublattice are not nearest neighbors on the original lattice) is an open and nontrivial question.[50] It would be very interesting to investigate the ordering type which occurs in the low-temperature regime encountered above. Similar to the 3-state AF Potts model with residual entropy on bipartite lattices for which some Monte Carlo simulations[35,36,40] indicate the existence of a broken sublattice symmetry (BSS) phase (where one spin state is favored on a sublattice and the remaining two states are favored on the other sublattice), one could expect such a type of ordering in the 4-state AF Potts model on the above tripartite fractal for $m\geq m_c$. In this case the BSS phase could be characterized, for example, by the predominance of one spin state in one sublattice, of another spin state in a second sublattice, and of the remaining two states in the third sublattice. Another possibility of ordering could be, as found by Adler *et al.*[51] for models governed by Hamiltonians with the same symmetries as those of the $q=3$ Potts antiferromagnet on a triangular lattice but with additional interactions, a phase with a partial order in which only the helicity symmetry is broken. This "helical" phase was also observed[52] in an AF classical XY model submitted to an external field on a tripartite lattice, but was not found on a bipartite lattice. A third possibility would be a phase with a null order parameter (where each site of a given sublattice would have equal probabilities of being occupied by any of the four-spin states). This was the case suggested by Ono's analysis[39] of his Monte Carlo simulations for the 3-state AF Potts model on the cubic lattice. The vanishing of the order parameter was also obtained[53] recently, by an *exact* procedure, for this model on a bipartite Migdal-Kadanoff-type HL. If one examines the probabilities, at $T=0$, of all the sites of the Sierpinski-gasket generator $G(4,1)$ to be occupied by a given state σ ($\sigma=1,2,3,4$), one can observe the tendency towards the equiprobability. We, therefore, consider this third possibility the most probable one.

4. *Critical exponents ν_T^{F} and ν_T^{AF} for $q=2$, 3, and 4*

The correlation-length critical exponents ν_T^{F} and ν_T^{AF} for the respective P-F and P-AF transitions are given by

$$\nu_T^s=\ln(b/b')/\ln\lambda_>^s \quad (s=\mathrm{F},\mathrm{AF}) , \tag{50}$$

where $\lambda_>^s$ is the greatest eigenvalue ($\lambda_>^s>1$) of the Jacobian matrix obtained through the derivation of the RG transformation with respect to the parameters evaluated at the semistable fixed point t_c^s ($s=\mathrm{F},\mathrm{AF}$).

The dependences of ν_T^{F} and ν_T^{AF} with $D_f(m)$ for the $q=2$-, 3-, and 4-state Potts model on the $(m\mathrm{SG})_4$ are shown in Figs. 13(a) and 13(b). It should be noted that ν_T^{F} diverges for $m\to 1$ as expected.[9] Its asymptotic behavior is given by

$$\nu_T^{\mathrm{F}}(q)\sim 1/[D_f(m)-D_f(1)], \quad m\to 1 , \tag{51}$$

which is similar to the result

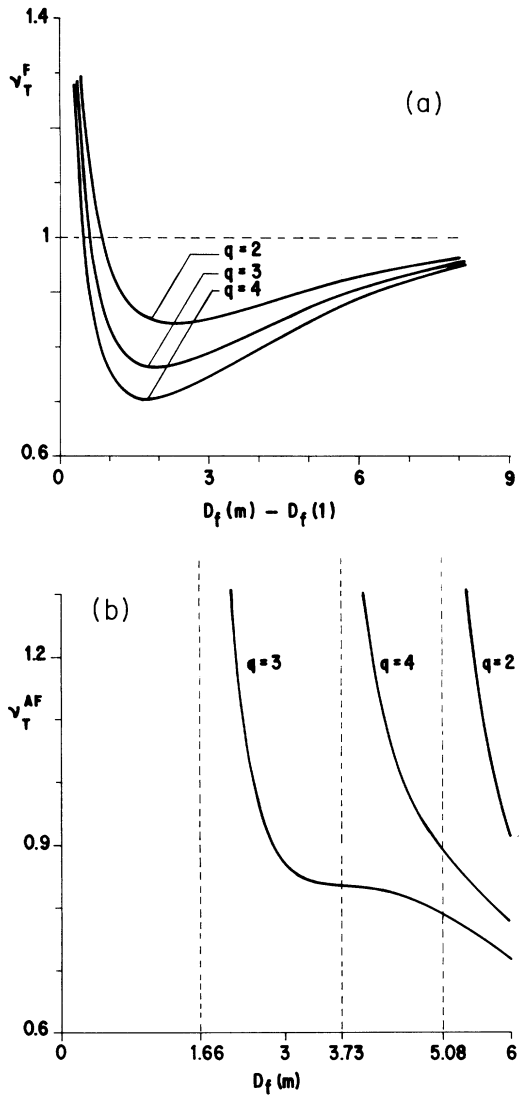

FIG. 13. The respective correlation-length critical exponents ν_T^F and ν_T^{AF} vs $D_f(m)$ for (a) para-ferromagnetic and (b) para-antiferromagnetic phase transitions. The asymptots represent the lower critical dimensions for different values of q.

$$\nu_T \sim 1/(d-1), \quad d \to 1$$

obtained for the Potts ferromagnet on hypercubic lattices[54] and Migdal-Kadanoff-like HL (Ref. 55) (where $d=1$ is the lower critical dimension for the P-F phase transition on these lattices). Similar to Ref. 55 (with $q>2$), the exponent ν_T^F presents, as a function of $D_f(m)$, a minimum at a value $D_f(m)=D_f^{\min}$ which increases for increasing values of q [see Fig. 13(a)]. In the $D_f(m)\to\infty$ limit, ν_T^F tends to 1 for all values of q, similar to the result obtained for Migdal-Kadanoff-like HL (Ref. 55) which differs from the behavior found for hypercubic lattices[56] where $\nu_T^F \to \frac{1}{2}$ $(d\to\infty)$.

For the P-AF transition, ν_T^{AF} diverges for $m=m_c(q)$ as a power law, namely,

$$\nu_T^{AF}(q) \sim D(q)[m-m_c(q)]^{-\theta(q)}, \quad m \to m_c(q), \qquad (52)$$

where $\theta(2)\cong 0.494$, $\theta(3)=1$, $\theta(4)\cong 0.511$, $D(2)\cong 7.00$, $D(3)=\ln 4$, and $D(4)\cong 2.20$.

Notice that the exact behavior of $\nu_T^{AF}(3)$ has the same form as that of Eq. (51).

VI. CONCLUSION

We have proposed families of deterministic fractals, the m-sheet Sierpinski gaskets with side b $[(m\mathrm{SG})_b]$, on which the q-state Potts model can be *exactly solvable* and which presents phase transitions at *finite* temperatures for $m>1$. Using a RSRG transformation which preserves under renormalization the ratios of the probabilities that the rooted spins are in fixed states, we obtained the *exact* para (P)–ferromagnetic (F) critical frontiers and the thermal correlation-length critical exponents, $\nu_T^F(m)$, as a function of m for the Ising model on the $(m\mathrm{SG})_2$ fractal family and for the $q=2$-, 3-, and 4-state Potts model on the $(m\mathrm{SG})_4$.

The RG transformation for the antiferromagnetic (AF) Potts model provides undesirable results on some cells of the $(m\mathrm{SG})_b$ for certain values of b like, for example, a renormalized ferromagnetic coupling in the first iteration which can lead to the appearance of a disconnected ferromagnetic phase. We have discussed this point and concluded that it occurs due to a failure in the preservation of the antiferromagnetic ground state of the chosen cells. Then, we proposed a criterion for a suitable choice of cells in the study of AF classical spin models defined on (or approximated by) multirooted hierarchical lattices. Applying this criterion, we verified that the fully frustrated AF Ising on the $(2\mathrm{SG})_2$ never orders (not even at $T=0$), similar to the triangular lattice. We also obtained the P-AF phase boundaries and their respective critical exponents $\nu_T^{AF}(m)$ for the $q=2$-, 3-, and 4-state AF Potts model on the $(m\mathrm{SG})_4$ family, which we expect to be the *exact* ones. In the cases where the ground state of this model is highly degenerated ($q=2$ and 4; in the $q=2$ case this degeneracy is due to frustration), an unusual low-temperature phase appears, above a certain critical fractal dimension $D_f^c(q,m)$, with an attractor at finite temperature. We have proved, for $q=2$, that such a phase is characterized by a power-law decay of correlations not only at the transition point, as usual, but throughout this entire phase. This result had already been suggested by Berker and Kadanoff[34] but, as far as we know, there has been no proof of this in the literature.

ACKNOWLEDGMENTS

During the early stages of this work we benefited from very fruitful discussions with Fa Y. Wu. We also acknowledge Evaldo M. F. Curado, Constantino Tsallis, and Paulo M. C. de Oliveira for useful remarks. We thank the Brazilian agency Conselho Nacional de Desenvolvimento Científico e Tecnológico (CNPq) for financial support.

[1]Y. Gefen, B. B. Mandelbrot, and A. Aharony, Phys. Rev. Lett. **45**, 855 (1980).
[2]Y. Gefen, A. Aharony, and B. B. Mandelbrot, J. Phys. A **16**, 1267 (1983).
[3]Y. Gefen, A. Aharony, Y. Shapir, and B. B. Mandelbrot, J. Phys. A **17**, 435 (1984).
[4]Y. Gefen, A. Aharony, and B. B. Mandelbrot, J. Phys. A **17**, 1277 (1984).
[5]R. Riera and C. M. Chaves, Z. Phys. B **62**, 387 (1986).
[6]R. Riera, J. Phys. A **19**, 3395 (1986).
[7]W. Zidan, G. Changde, and A. Holz, Phys. Rev. A **34**, 1531 (1986).
[8]U. M. S. Costa, I. Roditi, and E. M. F. Curado, J. Phys. A **20**, 6001 (1987).
[9]M. P. Grillon and F. G. Brady Moreira, Phys. Lett. A **142**, 22 (1989).
[10]T. Abe, J. Phys. Soc. Jpn. **58**, 1962 (1989).
[11]R. B. Stinchcombe, Phys. Rev. B **41**, 2510 (1990).
[12]R. B. Stinchcombe, Physica D **38**, 345 (1989).
[13]R. B. Griffiths and M. Kaufman, Phys. Rev. B **26**, 5022 (1982).
[14]M. Kaufman and R. B. Griffiths, Phys. Rev. B **24**, 496 (1981); **28**, 3864 (1983).
[15]J. R. Melrose, J. Phys. A **16**, 1041 (1983); **16**, 3077 (1983).
[16]B. Hu, Phys. Rev. Lett. **55**, 2316 (1985).
[17]E. P. da Silva and C. Tsallis, Physica A **167**, 347 (1990).
[18]J. Vannimenus, Z. Phys. B **43**, 141 (1981).
[19]M. Kaufman and R. B. Griffiths, J. Phys. A **15**, L239 (1982).
[20]P. M. Bleher and E. Zalys, Commun. Math. Phys. **120**, 409 (1989).
[21]M. Kaufman and R. B. Griffiths, Phys. Rev. B **26**, 5282 (1982).
[22]R. B. Griffiths and M. Kaufman, Phys. Rev. B **30**, 244 (1984).
[23]M. Kaufman, R. B. Griffiths, J. M. Yeomans, and M. E. Fisher, Phys. Rev. B **23**, 3448 (1981).
[24]J. M. Yeomans and M. E. Fisher, Phys. Rev. B **24**, 2825 (1981).
[25]C. Tsallis, A. M. Mariz, A. Stella, and L. R. da Silva, J. Phys. A **23**, 329 (1990).
[26]A. M. Mariz and C. Tsallis, Phys. Rev. B **32**, 6055 (1985).
[27]A. M. Mariz, A. C. N. de Magalhães, L. R. da Silva, and C. Tsallis, Physica A **162**, 161 (1990).
[28]F. Y. Wu, Rev. Mod. Phys. **54**, 235 (1982).
[29]C. Itzykson and J. M. Luck, in *Progress in Physics Vol. 11: Critical Phenomena,* edited by A. Jaffe, G. Parisi, and D. Ruelle (Birkhauser, Boston, 1985), p. 45.
[30]Y. Qin and Z. R. Yang, Phys. Rev. B **43**, 8576 (1991).
[31]G. S. Grest, J. Phys. A **14**, L217 (1981).
[32]F. Y. Wu, J. Stat. Phys. **23**, 773 (1980).
[33]G. H. Wannier, Phys. Rev. **79**, 357 (1950).
[34]A. N. Berker and L. P. Kadanoff, J. Phys. A **13**, L259 (1980).
[35]J. R. Banavar, G. S. Grest, and D. Jasnow, Phys. Rev. Lett. **45**, 1424 (1980).
[36]G. S. Grest and J. R. Banavar, Phys. Rev. Lett. **46**, 1458 (1981).
[37]W. Kinzel, W. Selke, and F. Y. Wu, J. Phys. A **14**, L399 (1981).
[38]M. P. Nightingale and M. Schick, J. Phys. A **15**, L39 (1982).
[39]I. Ono, Prog. Theor. Phys. Suppl. **87**, 102 (1986).
[40]J. S. Wang, R. H. Swendsen, and R. Kotecky, Phys. Rev. Lett. **63**, 109 (1989).
[41]R. Hilfer and A. Blumen, J. Phys. A **17**, 1537 (1984).
[42]Z. Borjan, S. Elezović, M. Knežević, and S. Milošević, J. Phys. A **20**, L715 (1987).
[43]P. Alstron, D. Stassinopoulos, and H. E. Stanley, Physica A **153**, 20 (1988).
[44]S. Elezović, M. Knežević, and S. Milošević, J. Phys. A **20**, 1215 (1987).
[45]T. Stošić, B. Stović, S. Milošević, and H. E. Stanley, Phys. Rev. A **37**, 1747 (1988).
[46]B. B. Mandelbrot, *The Fractal Geometry of Nature* (Freeman, New York, 1983).
[47]A. Bakchich, A. Benyoussef, and N. Boccara, J. Phys. C **3**, 1727 (1991).
[48]C. Tsallis and S. V. F. Levy, Phys. Rev. Lett. **47**, 950 (1981).
[49]P. M. C. de Oliveira, J. Phys. (Paris) **47**, 1107 (1986).
[50]A. V. Bakaev, V. I. Kabanovich, and A. M. Kurbatov, Int. J. Mod. Phys. B **5**, 3061 (1991); J. Phys. A **25**, L31 (1992).
[51]J. Adler, Y. Gefen, M. Schick, and Wei-Heng Shih, J. Phys. A **20**, L227 (1987).
[52]D. H. Lee, R. G. Caflisch, J. D. Joannopoulos, and F. Y. Wu, Phys. Rev. B **29**, 2680 (1984).
[53]J. A. Redinz, E. M. F. Curado, and A. C. N. de Magalhães (unpublished).
[54]M. J. Stephen, Phys. Lett. **56A**, 149 (1976).
[55]L. R. da Silva and C. Tsallis, J. Phys. A **20**, 6013 (1987).
[56]K. G. Wilson and M. E. Fisher, Phys. Rev. Lett. **28**, 24 (1972).

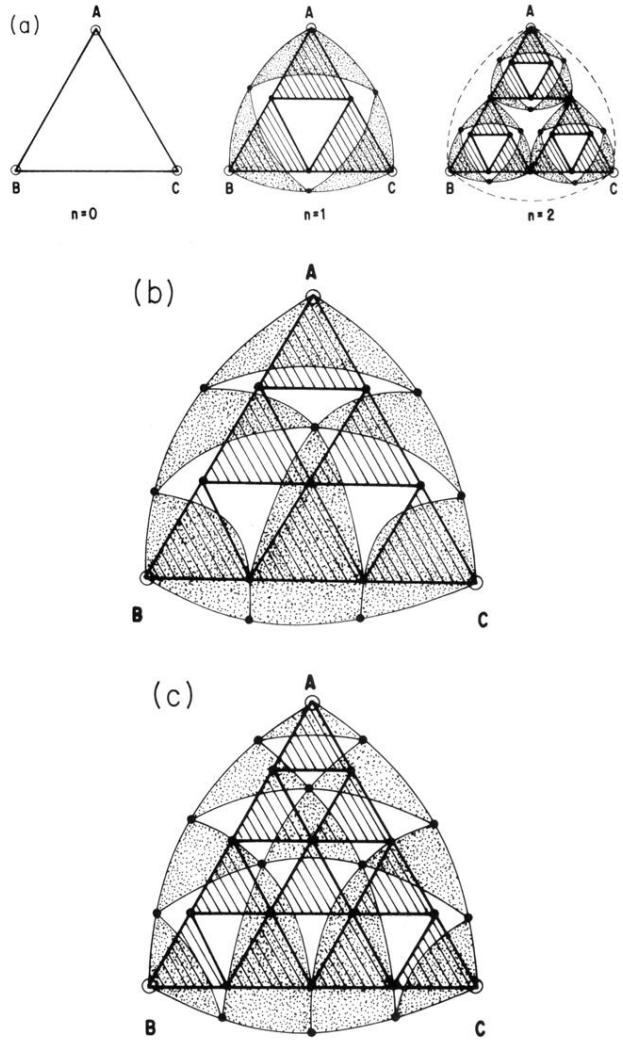

FIG. 1. (a) The first three stages (n) of construction of the $(2SG)_2$ fractal. The second sheet of the $n=2$ stage connected to A, B, and C is represented by just a single dashed line for visual purposes. (b) The generator ($n=1$) stage of the $(2SG)_3$. (c) The generator of the $(2SG)_4$. The roots and internal sites are represented by open and solid points, respectively.